Available online at www.sciencedirect.com

ScienceDirect

Advances in Space Research 70 (2022) 601–609

ADVANCES IN SPACE RESEARCH (a COSPAR publication)

www.elsevier.com/locate/asr

Modeling of Ka-band slant path rain attenuation for hilly tropical region

Swastika Chakraborty [a], Pooja Verma [b], Bishal Paudel [b], Saurabh Das [c,*]

[a] Narula Institute of Technology, 81, Nilganj Road, Agarpara, Kolkata 700109, India
[b] Sikkim Manipal Institute of Technology, Sikkim, India
[c] Department of Astronomy, Astrophysics and Space Engineering, Indian Institute of Technology, Khandwa Road, Simrol, Indore 453552, India

Received 22 May 2021; received in revised form 23 March 2022; accepted 1 May 2022
Available online 7 May 2022

Abstract

Experimental measurement of satellite signal at 20.2 GHz using GSAT-14 satellite beacon has been carried out over the hilly tropical location Umiam, Shillong during 2017–2019. Collocated rainfall measurements have been done using a laser precipitation monitor for the same duration. The data have been analyzed to understand the signature of orographic rainfall on the Ka-band signal and to achieve the highest possible reliability of signal reception for a high rainfall tropical location. Complementary cumulative distribution of experimentally obtained rain attenuation is compared with that of conventional ITU-R model calculated rain attenuation and recently developed Chang Sheng model predicted rain attenuation values. The result shows severe overestimation of the actual measurement by both the ITU-R model and Chang Sheng model. The Chang Sheng model is further modified with the orographic adjustment factor for predicting orographic rain attenuation. The model was developed based on the data of 2017–18 and validated using the measured attenuation of the year 2019. The performance of the proposed model is evaluated in terms of RMSE and correlation coefficient. The value of the correlation coefficient has been found to be 0.988, and the RMSE value has been found to be around 3.0986, which indicates the acceptable performance of the proposed model. The proposed model is further optimized for operational elevation angle range, rain rate range, and frequency range. The proposed model will help in optimizing the power utilization in the Uplink Power Control technique for rain attenuation mitigation over high rainfall hilly regions.

Keywords: Orographic rain; Ka-band; Rain attenuation; Terrain gradient; Non-monotonic behavior

1. Introduction

Increasing use of broadband satellite services calls for the use of higher frequency bands (>10 GHz) to overcome the spectral congestion at lower frequency bands. The use of higher frequency bands also makes possible miniaturization of equipment dimensions. However, Ka-band frequencies are seriously affected during rain and are a serious concern for high rainfall regions.

In this respect, experimental studies have been carried out mainly over temperate locations and very few tropical countries due to the limited availability of experimental beacon measurement at these frequencies. Kubista (Kubista et al., 2000) showed that there was a wide variation of signal availability over urban, semi-urban, and tree-shadowed regions of Germany, Austria, Netherland, and France based on the cumulative distribution function of the received signal from the ITALSAT satellite at 18.7 GHz at 28° and 36° elevation angles. In another study, three years of experimental measurements of beacon signals at the frequency 20.185 GHz and 27.505 GHz have

* Corresponding author.
E-mail address: das.saurabh01@gmail.com (S. Das).

https://doi.org/10.1016/j.asr.2022.05.002
0273-1177/

been done as a part of the NASA ACTS experiment over eight different locations in the USA (Feldhake and Sengers, 2002). It was concluded that the ITU-R model-based DAH model (Dissanayake et al., 1997) and radar measurement-based Excell model (Luini and Capsoni, 2011) show, in general, 30% to 40 % errors while comparing with the experimental result. On the contrary, using three years of experimental measurement at 20 GHz over eight stations of North America, (Tjelta et al., 2017) found that the ITU-R model (Rec. ITU-R P.618-12, 2015) performs satisfactorily well for most of the time and even at the low elevation angle of 3.2°.

Over the location Singapore, after analyzing beacon signals at 18.9 GHz (Yeo et al., 2014) from WINDS and GE23 satellite; a model was proposed and compared with several existing models like Yamada (Yamada et al., 1987), Dissanayake (Dissanayake et al., 1997), and Ramachandran (Ramachandran and Kumar, 2007). The proposed model was found to outperform the existing models compared. Recently, (Changsheng et al., 2018) proposed a slant-path rain attenuation prediction model considering the non-monotonic behavior of rain attenuation with the elevation angle and the rain rate. ITU-R model predicted attenuation (Rec. ITU- R P.838-3, 2005, Rec. ITU-R P.618-13, 2017) was also compared (Samat et al., 2019) with the experimental results over Malaysia using beacon signal from MEASAT-5 at frequency 20.2 GHz. ITU-R model was found to overestimate the experimental attenuation values over that location. The author indicated that the discrepancy might be due to the large antenna size and the high elevation angle of 68°. Over the tropical coastal region of Thiruvananthapuram (8.5°N, 76.8°E), the Ka-band satellite signal from GSAT-14 was tracked and characterized (Mishra et al., 2020). This study has been evaluated with the ITU-R model (Rec. ITU- R P.838-3, 2005). It was found that the ITU-R model estimated attenuation did not match with measured attenuation over this location.

In the absence of beacon measurement, the variability of rain attenuation has been studied from the raindrop size distribution (Maitra., 2004, Das et al., 2010) for the range of frequency 10–200 GHz over different tropical locations. Further, the rain attenuation distribution has been studied over other tropical areas for the range of frequency 1–1000 GHz using Mie scattering and Liebe's dielectric model (Mulangu and Afullo, 2009). Over the tropical locations, some indirect radiometric measurements were also available (Karmakar et al., 2000) for rain attenuation prediction at 22.235 GHz and 31.4 GHz. Forty years of rainfall data from different sites of Bangladesh (Begum and Ifiok, 2008), a tropical country, have been used along with Rice- Holmberg model (Rice and Holmberg, 1973) to find the rain rate and the attenuation, based on the ITU-R model (Rec. ITU-R P.618-8, 2003). The existing rain attenuation model was then modified for predicting attenuation at 18.7 GHz using the beacon measurement of Sparsholt, U.K.

Existing models of rain attenuation, as given by (Flavin, 1996) and (Dissanayake et al., 1997), cover a wide frequency range from 4 GHz to $\sim$ 60 GHz. However, the attenuation prediction was consistently underestimated while validating the experimental result over the tropical regions. In recent years, the parabolic equation model (Sheng et al., 2014) was developed at the millimeter wave frequency band for rain attenuation prediction. It was shown to be successful in considering the uncertainty in the physical conditions over a satellite link. A simulation (Panchal and Joshi, 2016) study over different Indian locations based on ITU-R model(Rec. ITU-R P.618-12, 2015), SAM model(Stutzman and Yon, 1986) and Garcia Lopez model (García-López et al., 1988) has shown that each model has acceptable performance for a specific range of rain rate and operating frequency as well depend on the climate of that region.

The previous studies indicate that above 10 GHz satellite link design is very sensitive to the elevation angle and the rain rate. Several rain attenuation prediction models indicate a non-monotonic behavior with the elevation angle as indicated in the (ITU-R recommendation, 2003; Rec. ITU-R P.618-12, 2015), Brazil model (Rec. ITU-R Doc. 3M/17, P.618-7, 2003) and in other literature (Mello and Pontes, 2012)). However, this is not in accordance with the actual measurements. Further, predicted rain attenuation has been found to vary non-monotonically with the rain rate for low latitude (within 36°S and 36°N) and especially for the low elevation angle within 25° (Rec. ITU-R Doc. 3J/50, P.618-9, 2008) which is again not supporting the actual measurement. A very recent model (Changsheng et al., 2018) especially developed for the low latitude (36°N – 36°S) and the elevation angle (<25°), takes care of the non-monotonic behavior of attenuation with the elevation angle and the time percentage. This model proposes an adjustment term for the rainfall rate considering the exponential profile of the rain cell. The exponential profile of rain cells accounts for the non-uniform rain rate distribution in space and time. The rain rate adjustment factor in this model is calculated using a simulated annealing algorithm (SAA), Genetic algorithm (GA), and ITU-R DBSG3 database. This model has outperformed other existing models above 10 GHz for a wide range of frequencies, latitudes, and elevation angles.

Another critical issue in rain attenuation studies is that the majority of these studies were carried over the plain locations, and there are very few studies of the propagation impairment have been attempted over the hilly locations. Recently, (Debnath et al., 2017) found that the ITU-R model (ITU-R P.838-3, 2005) predicted attenuation matches well with the experimental data at Ka-band frequency only at the high end of attenuation over Shillong, a hilly location. The presence of a hill causes a significant impact on the rainfall pattern and leads to an enhancement of rainfall intensity. Therefore, signal attenuation due to rainfall over hills needs special attention. Rain attenuation at the hilly terrain is not only modified by terrain type but

also by the background precipitation intensity, the effect of which, in turn, is reflected on path length. It can cause long-duration attenuation, which can be addressed by including orographic modification to the rain attenuation. At the Ka band, where attenuation is significantly higher than the Ku band, reliable prediction is difficult to achieve without proper modification of attenuation considering orography. The path integrated attenuation method is unstable towards the high attenuation range. Moreover, radar data has limited performances over hilly regions as reflections of the signal at the hill (Gray and Seed, 2000), and the earth's curvature may affect the measurement. Also, radar often scans above the region where orographic transformation occurs. Therefore, reliable models based on ground-based measurement are essential for the satellite communication link designers, even for the hilly locations.

This paper primarily attempts to characterize rain patterns over the hills and proposes a further modification of the Chang Sheng model for rain attenuation prediction over the hilly region. The following section describes the ITU-R model for rain attenuation prediction and the modification proposed in the Chang Sheng model.

2. Rain attenuation models

2.1. ITU-R rain attenuation model

This model (ITU-R P.838-3, 2005) considers point rain rate distribution and assumes a uniform spatial rainfall structure. Percentage exceedance of rain attenuation for 0.01% of the time is modeled as.

$$A_{0.01} = YL_E \tag{1}$$

where specific attenuation is denoted by Y and L_E is path length covered by rain.

Again specific attenuation is given by:

$$Y = KR_{0.01}{}^{\alpha} \tag{2}$$

K and α are frequency-dependent coefficients, $R_{0.01}$ is the rain rate exceeded 0.01% of an average year.

However, neither temporal nor spatial profile of the rain rate is uniform. ITU-R model (ITU-R P.838-3, 2005) shows a non-monotonic variation with elevation angle (Changsheng et al., 2018), rain rate, and time percentage, especially for low latitude and low elevation angle.

2.2. Chang Sheng rain attenuation model

To account for the above limitation of the ITU-R model (ITU-R P.838-3, 2005), Chang Sheng rain attenuation model used the path adjustment factor (r_{eff}) of the Crane model (Crane, 1980),

$$r_{eff} = \frac{\bar{R}}{R(p)} \tag{3}$$

$\bar{R}$ is average rain rate over satellite path and R(p) is the rain rate at a time percentage p. It considers the rain cell profile of the EXCELL (Luini and Capsoni, 2011) model and the HYCELL(Feral et al., 2003) model to address spatial non-homogeneity of rain. The rain rate distribution along the slant path is given by

$$R(x,p) = R_{max}(p)e^{-b|x-L_D|} \tag{4}$$

where R(x, p) is the percentage exceedance of rainfall rate for p% of time at a distance $x \times$ from the receiver. R_{max} (p) is the maximum rain rate for p% of an average year along the horizontal projection in (mm/h), L_D(km) denotes the distance between the maximum rain rate location and the location of the observation site. b is the inverse of equivalent radius at the point where rain-rate falls by 1/e, i.e.

$$R = \frac{Rmax}{e} \tag{5}$$

Assuming the majority contribution by only one cell for simplicity, Eq. (3) is modified as.

$$Rmax(p) = R(0,p)e^{bL_D} = R_0(p)e^{bL_D} \quad mm/hr \tag{6}$$

where $R_0 = R(0,p)$

Now from Eq. (2).

$$Y = KR_{0.01}{}^{\alpha}$$

K and α are frequency-dependent coefficients, $R_{0.01}$ is rain rate exceeded 0.01% of an average year.

Exceedance of attenuation during p% time is calculated as follows:

$$A(p) = \int_0^{Ls} kR(l\cos\theta.p)^{\alpha}dl \tag{7}$$

$$= k[R_0(p)]^{\alpha}(Ls\delta) \tag{8}$$

where $[R_0(p)] = .\int_0^{L_s} R(l\cos\theta.p)$

where Ls is the length of the slant path, θ is the elevation angle, and δ is the path adjustment factor.

The path adjustment factor is given by.

$$\delta = \frac{2b\alpha L_D}{b\alpha LsCos\theta}\left[1 - e^{-b\alpha L_G}\right] \tag{9}$$

L_G(km) denotes the distance between rain rate at rain height location and observation site.

Applying Taylor series expansion of exponential term of Eq. (9).

$$1 - exp^{-b\alpha L_G} \approx b\alpha L_s \cos\theta \tag{10}$$

Using Eqs. (4), (9), and (10), attenuation exceedance for p% of time is modified as.

$$A_{ChangSheng} = A(p) = k[r(p)R(p)]^{\alpha} Ls \tag{11}$$

where R(p) is the rainfall rate for p% average exceedance.

The adjustment factor of rain rate (Changsheng et al., 2018) is given by.

$$r(p) = r_1(p)r_2(p) \tag{12}$$

$$\text{where} \quad r_1(p) = a_1 R(p)^{a_2 + \frac{a_3}{Ls}} \tag{13}$$

$$\text{and} \quad r_2(p) = 1 + \frac{a_4 P^{a_5}}{1 + a6Ls} \tag{14}$$

The coefficients $a_1, a_2\, a_3\,, a_4, a_5\,, a_6$ are obtainable from previously mentioned algorithms (Changsheng et al., 2018) and the ITU-R DBSG3 database.

Finally, putting the value of $r_1(p)$ and $r_2(p)$ in Eq. (12) rain rate adjustment factor comes as.

$$r(p) = 3.78R(p)^{-0.56+\frac{1.51}{Ls}}\left(1 - \frac{0.85p^{0.065}}{1 + 0.12Ls}\right) \tag{15}$$

This model shows monotonic behavior of the predicted attenuation with time percentage, rate of rainfall, and elevation angle for a maximum 60 GHz frequency.

3. Experiment description

GSAT-14 satellite signal is tracked at Umiam (25.6768° N, 91.9270° E), North Eastern Space Application Center (NESAC), ISRO, Shillong at an elevation angle of 58.53°. The data is collected for the year 2017–2019 with the help of a beacon receiver, VSAT antenna (horizontal polarization) of 0.6-meter diameter, and data recording software with a rate of sampling of 10 Hz. The signal is received at a frequency of 20.2 GHz. GSAT-14 transmits linear polarization signal from geostationary orbit at 74° E with an EIRP of 24 dBW. The actual instruments and the block diagram of the experimental setup are shown in Fig. 1(a) and Fig. 1(b). After reception of the signal, it is down-converted through L-Band down converter after low noise block converter, and then it is received through the digital receiver. The signal is then processed at the host computer. The station height here is 1.5 km (Das and Maitra, 2016) above mean sea level, and 0° isotherm height is 4.7573 km according to ITU-R recommendation (ITU-R P.839-3, 2001).

Collocated rainfall data is collected through Laser Precipitation Monitor (LPM) at NESAC with a temporal resolution of one minute. This experimental setup is the result of the collaboration of ISRO with CNES/ONERA.

3.1. Location of the study

Umiam, Shillong (25.6768°N, 91.9270°E) is located at about 1.5 km (Das and Maitra, 2016) altitude, where the humid climate is prevalent throughout the year. Specifically, the annual average rainy days of Shillong is about 130, with an annual average total rainfall amount is approximately 3385 mm.

3.2. Pre-processing of rainfall data and associated radio signal data

Event-wise rainfall rate and radar reflectivity data are extracted from the LPM at Umiam, Shillong, for 2017–2019. The receiver signal is considered for the analysis based on the rainy days of LPM data. Voltage level corresponding to analog signal from the receiver at 20.2 GHz is getting digitized with the help of analog to digital converter (ADC) (make National Semiconductors ADC083000)). Finally, the signal is transformed into dB after necessary signal processing. ADC has a sample rate of (2x) 1.45 to 1.8 GHz, bit resolution of 8 bit (−127 to +128), and a full power bandwidth of 0.1 GHz to 1.5 GHz.

The received signal is then filtered with a 10th order Butterworth low pass filter with a cut-off frequency of 0.025 Hz (Matricciani, 2008) to remove the fast fluctuation i.e., scintillation. The difference of measured signal and reference level is taken as attenuation.

The pre-processing starts (Das et al., 2020) with the segregation of rainy and non-rainy days from the available data of 2017, 2018, and 2019. Rainfall data availability of 2017, 2018, and 2019 are 40%, 83.3%, 41.6%, respectively. To observe the clear air variation of signals, the non-rainy days of each monsoon month, approximately 10–11 days, are segregated. This segregation is done for

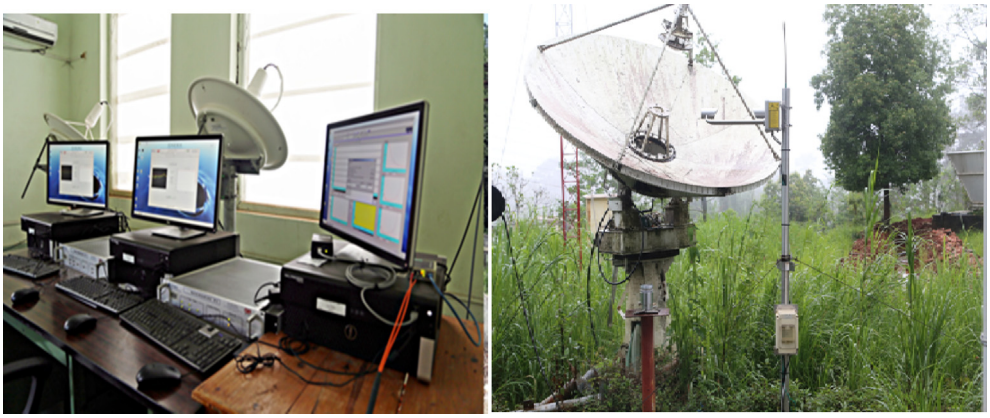

Fig. 1a. Snapshot of experimental setup for Shillong.

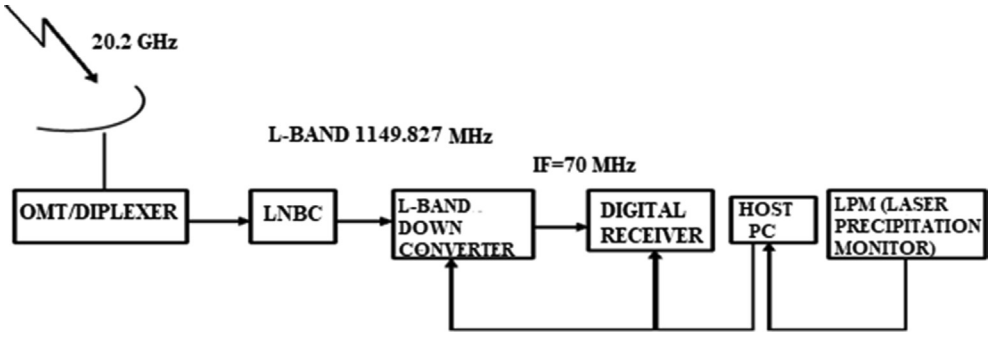

Fig. 1b. Block diagram of the experimental setup.

each month of the available year 2017, 2018, and 2019. In the next step, for each month, non-rainy signal level values are separately averaged before filtering. Then for removing scintillation, further processing of average non-rainy signal level has been done by filtering with the same cut-off frequency. Now the clear sky signal, or in other words, non-rainy days signal, is used as a reference signal level for the calculation of attenuation (dB) for that particular month. Finally, total attenuation is considered the difference of reference signal level (dB) from the measured signal level (dB) at the time of rain. Cloud attenuation is not separately considered over here. Rain attenuation at this frequency can be approximated as total attenuation as the contribution to attenuation due to rain is much more compared to the attenuation due to other atmospheric constituents.

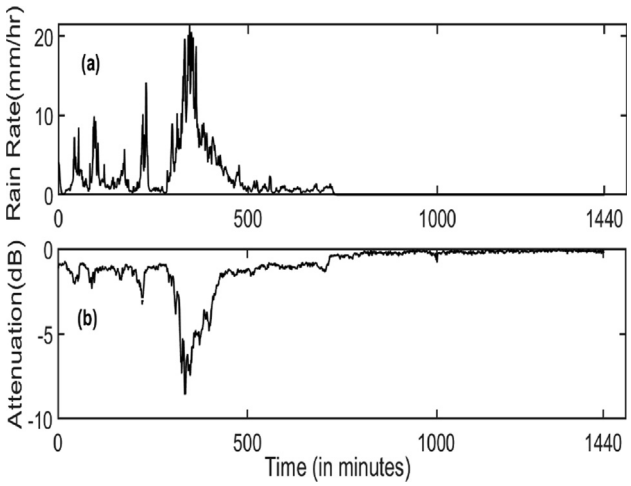

Fig. 2. (a) Rain rate and (b) rain attenuation at 20.2 GHz at Umiam, Shillong on 13th June 2018.

4. Results

4.1. Performance comparison of existing rain attenuation model

Elevation angle adjustment in the signal reception at a hilly terrain is a major issue for a reliable satellite link design. Moreover, non-homogeneity of the rain rate in space and the time significantly influence attenuation caused by rain in the hilly region. ITU-R rain attenuation model (Rec. ITU-R P.837-4, 2003) and some other popular models of rain attenuation show non-monotonic behavior of attenuation in relation to the time and the rain rate at low latitude region (within 36°N and 36°S) and below 25° elevation angle (Changsheng et al., 2018). Fig. 2 depicts the rain rate of an event of 13th June 2018 and its corresponding attenuation at 20.2 GHz. Here Chang Sheng model (Changsheng et al., 2018) and commonly used ITU-R model (ITU-R P.838-3, 2005) predicted attenuation are compared in terms of complementary cumulative distribution function (CCDF) in Fig. 3 with experimental measurement of attenuation at 20.2 GHz over Umiam, Shillong for the year 2017 and 2018. The result shows severe overestimation of the actual measurement by both the ITU-R model and the Chang Sheng model.

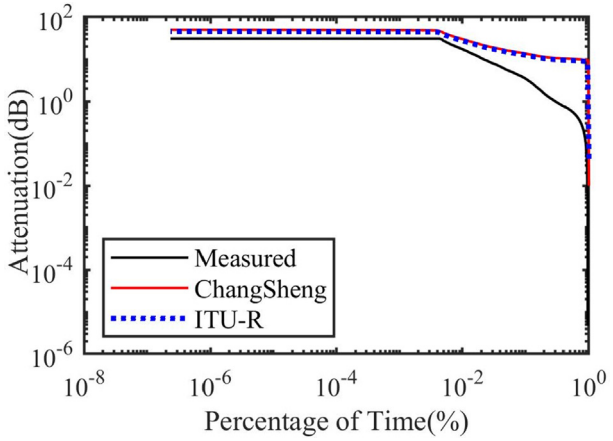

Fig. 3. Complementary cumulative distribution of rain attenuation at 20.2 GHz for the events of the years 2017 and 2018. ITU-R model and ChangSheng model calculated attenuation over Umiam, Shillong at the same frequency are also shown for comparison.

Most of the models used so far have already shown the non-monotonic behavior of attenuation with elevation angle. In addition to this problem within low latitude (within 36°S and 36°N) and low elevation angle (within 25°), attenuation shows non-monotonic behavior with the

rain rate and the percentage of the time. The Chang Sheng model has considered all these factors and introduces a rain rate adjustment factor to improve the existing models. Therefore Chang Sheng model is used here for comparison with the measured data, and the ITU-R model (ITU-R P.838-3, 2005) predicted attenuation.

The overestimation by Chang Sheng model is due to the change in rain attenuation pattern by orographic influence due to the presence of hills over this location. An attempt is made in this study to address the issue with the insertion of an orographic adjustment factor in rain attenuation prediction. This may prevent unnecessary power wastage at the time of link design.

4.2. Proposed model of rain attenuation for hilly region

Rain attenuation due to orography is therefore separately considered in the proposed model by introducing an orographic adjustment factor. Chang Sheng model already considers the probable factors like length of the slant path, the distance between receiver and the location of maximum rain rate, the path averaged rain rate, surface point rain rate, the latitude and the longitude of station, the elevation angle, the polarization tilt angle and the station height. The recent improvement of the ITU-R model i.e., Chang Sheng model as defined by equation (11), is taken as the base model for proposed model development. Due to the presence of hills in the present study location, the background precipitation intensity differs from the plain location. Therefore the rainy path length changes compared to that have been assumed by the Chang Sheng model over the plain location. Here an attempt has been made to adjust the path length of the Chang Sheng model and to fit with the experimentally measured complementary cumulative distribution function (CCDF). The equation is further modified in the following way to account for the orographic rain of the hilly region as follows:

$$A_{improved} = k[r(p)R(p)]^{\alpha}\, 0.48 * Ls - (3.949\exp^{0.5322p} - 10.96\exp^{-90.56p} \quad (16)$$

The above equation is based on the experimentally received signal from the GSAT-14 satellite of two years (2017 to 2018) of measurement over Shillong (25.5°N, 91.8°E). Fig. 4 shows the experimental value of the attenuation for the years 2017 and 2018 along with the fitted model for Umiam, Shillong. From the figure, there is a very good match is observed in between the fitted curve and the measured data of 2017 and 2018.

4.3. Performance of the proposed model

Fig. 5(a) and Fig. 5(b) show the proposed model predicted attenuation time series along with measured time series of 11th June 2019 and 8th July 2019. Fig. 6 shows the proposed model predicted attenuation complementary cumulative distribution function for 2019 with the mea-

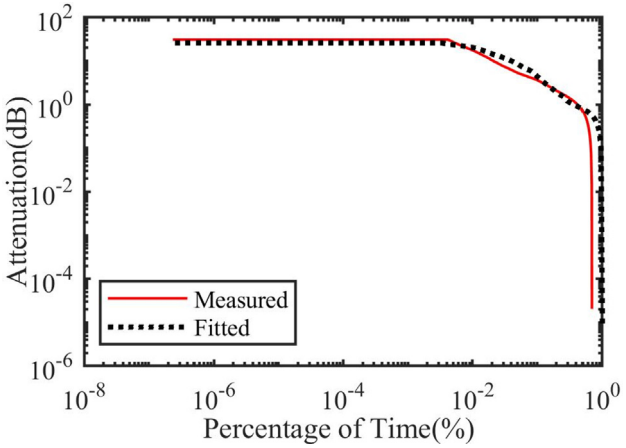

Fig. 4. Complementary cumulative distribution of experimentally measured rain attenuation at 20.2 GHz of the year 2017–2018 and the fitted curve.

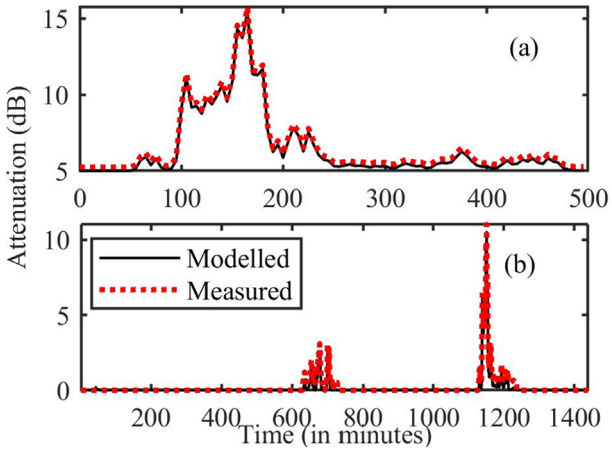

Fig. 5. Time series of experimentally measured rain attenuation at 20.2 GHz and proposed model predicted attenuation for (a) 11th June 2019 and (b) 8th July 2019.

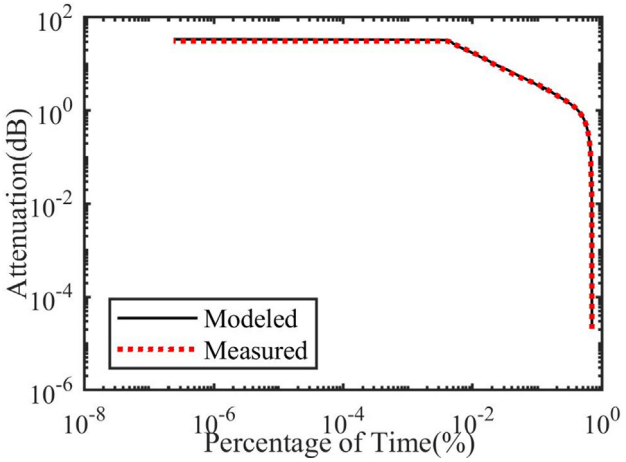

Fig. 6. Complementary cumulative distribution of experimentally measured rain attenuation at 20.2 GHz compared with developed model calculated attenuation for the year 2019.

sured attenuation. Up to 0.01% of time, there is a good match of the proposed model with experimental data and after that there is a very slight mismatch has been found. This mismatch may be due to not considering cloud attenuation separately which can be significant in Ka-band and for heavy convective clouds. However, the root mean square error (RMSE) and correlation coefficient between the proposed model and experimentally measured value shown in Table 1, indicates a good agreement between the proposed model and the experimental data. Fig. 7 shows the variation of the orographic adjustment factor with the variation of percentage of the time. This projection may be helpful for the prediction of attenuation over the hilly tropical location.

Along the gradient of the hill, low elevation angle causes severe attenuation, which can't be measured due to the lack of experimental facility. Scaling of attenuation based on the elevation angle can solve this issue partially. The variation of attenuation at 40 GHz earth space link predicted by the newly developed model with the angle of elevation at different rainfall rates is shown in Fig. 8. Attenuation shows a nearly monotonic relation with the elevation angle indicating higher attenuation at higher rain rate up to 80 mm/hr, which conforms to the behavior shown in Chang Sheng model.

Table 1
Quantitative prediction errors between proposed model predicted attenuation and experimentally measured attenuation.

Year	RMSE	Correlation Coefficient
2019	3.0986	0.988

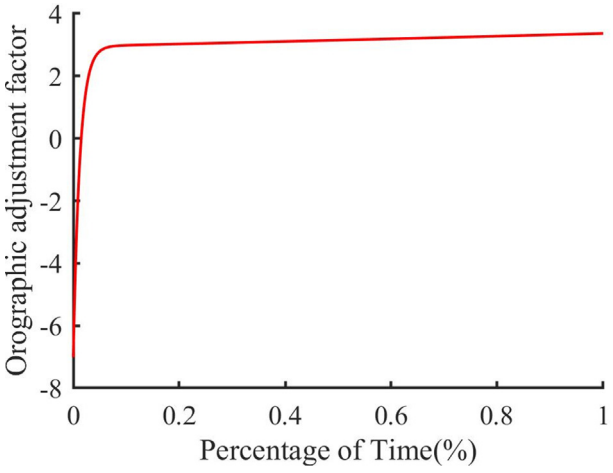

Fig. 7. Variation of orographic adjustment factor with percentage of time.

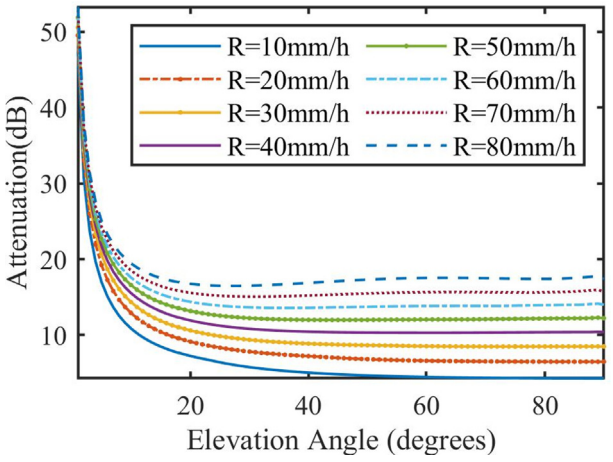

Fig. 8. Rain attenuation variation calculated by proposed model with different elevation angle for rain rate 10 mm/hr to 80 mm/hr at frequency 40 GHz.

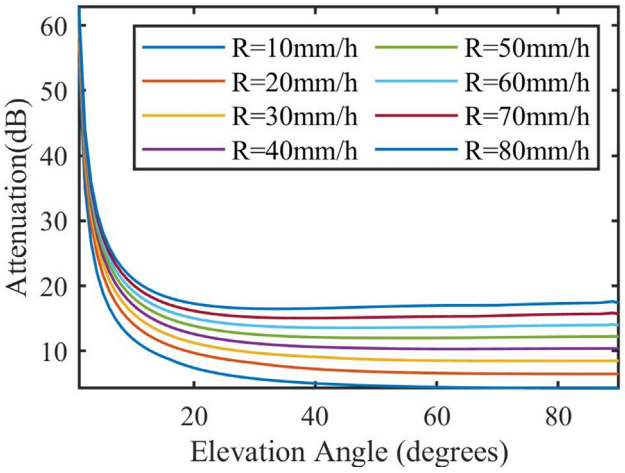

Fig. 9. Rain attenuation variation calculated by proposed model with different elevation angle for rain rate 10 mm/hr to 80 mm/hr at frequency 60 GHz.

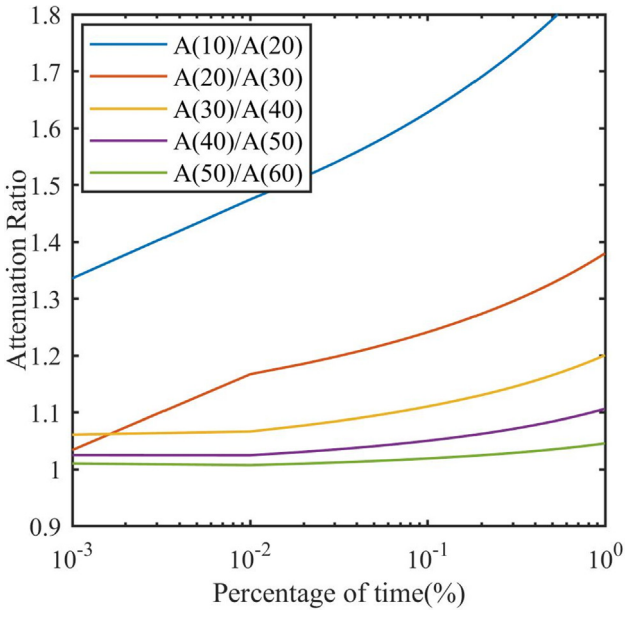

Fig. 10. Variation of attenuation ratio calculated by proposed model with different elevation angle for rain rate 50 mm/hr and at frequency 26 GHz.

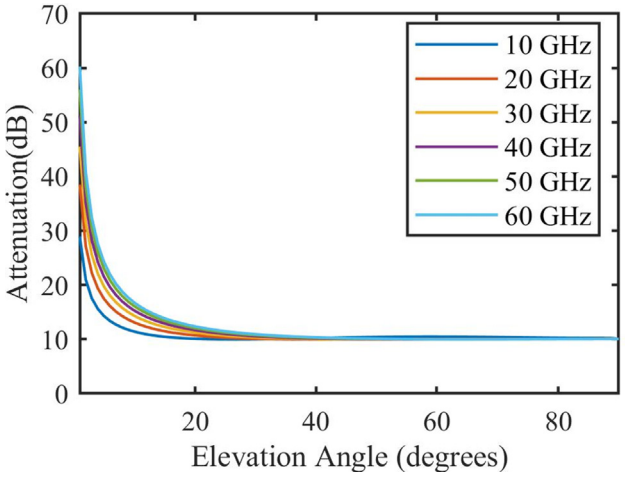

Fig. 11. Variation of attenuation with elevation angle at rain rate 40 mm/hr for different frequencies.

The performance of new model is further tested in Fig. 9 for higher frequencies. It can be concluded from Fig. 9 that at 60 GHz, attenuation varies monotonically with the elevation angle for a wide rain rate range (10–80 mm/hr.).

For a typical frequency of 26 GHz and rain rate 50 mm/hr., attenuation ratios for different elevation angles have been plotted in Fig. 10. Attenuation ratio means here the ratio of the low elevation angle attenuation and the high elevation angle attenuation. Its value greater than one confirms the expected higher attenuation in low elevation angle, which is not always true in the ITU-R model (Changsheng et al., 2018). This improvement of the ITU-R model found in the Chang Sheng model is retained in the proposed model.

The predicted attenuation for frequency ranges from 10 GHz to 60 GHz is shown in Fig. 11. Given the present commercial demand of 20 GHz frequency band and considering the gradual demand of higher frequency bands in the near future, the proposed model can help in frequency scaling of attenuation when only low-frequency attenuation data is available for low elevation angle range up to 20°.

5. Conclusion

An improvement over the latest modification of the ITU-R model i.e., Chang Sheng model, is carried out to account for the orographic contribution in rain attenuation at 20.2 GHz. As the hilly terrain is prone to rainfall due to updraft of wind across the hills and due to the random nature of elevation in hill topography, experimental study over this region is essential before the satellite link design for commercial purposes. The model is developed based on two years (2017–18) of experimental data and validated against the year 2019. The proposed model predicted attenuation is found to show monotonic behavior with the variation of elevation angle, rain rate, and frequency for high-frequency operation. The proposed model is found to have a correlation coefficient of 0.988 and RMSE of 3.0986 while comparing the model with separate one year of data of this particular place. The proposed model is also optimized for the specific elevation angle range, the rain rate range, and the frequency range. The proposed model is useful in efficient power utilization in link designing for this high rainfall hilly region, particularly for the uplink power control (ULPC) system. However, further validation of the proposed model over several hilly regions is required to reconfirm the performance of the proposed model.

Declaration of Competing Interest

The authors declare that they have no known competing financial interests or personal relationships that could have appeared to influence the work reported in this paper.

Acknowledgements

Authors thankfully acknowledge the scientists of Space Applications Center, ISRO for providing the experimental data. Financial support received under ISRO-RESPOND program and TMA Pai research grant are also thankfully acknowledged.

References

Begum, S., Ifiok, O., 2008. Characterization of rain attenuation in Bangladesh and application to satellite link design. Radio Sci. 43. https://doi.org/10.1029/2007RS003634.

Crane, R.K., 1980. Prediction of attenuation by rain. IEEE Trans. Communication. 28 (9), 1717–1733.

Changsheng, L., Zhao., Zhen, W., Leke, L., Phunsak, T., & Xin, Z., Zhao-Feng, L., 2018. A New Rain Attenuation Prediction Model for the Earth-Space Links. IEEE Trans. Antennas Propagat., 66: 5432–5442.

Dissanayake, A., Allnutt, J., Haidara, F., 1997. A prediction model that combines rain attenuation and other propagation impairment along earth-satellite paths. IEEE Trans. Antennas Propagat. 45, 1558–1564.

Da Silva, M.L.A.R., Pontes, M.S., 2012. Unified method for the prediction of rain attenuation in satellite and terrestrial links. J. Microwaves Optoelectron. Electromagn. Appl. 11 (1), 1–14.

Debnath, A., Das, R.K., Gogoi, D., 2017. A study of Ka-Band Signal Attenuation at Umiam, Meghalaya with ISRO's GSAT-14 Satellite. ADBU-J. Eng. Technol. 6 (2), 7–10.

Das, S., Maitra, A., 2016. Vertical profile of rain: Ka band radar observations at tropical locations. J. Hydrol. 534, 31–41. https://doi.org/10.1016/j.jhydrol.2015.12.053.

Das, S., Maitra, A., Shukla, A.K., 2010. Rain Attenuation Modeling in the 10–100 GHz Frequency Using DROP Size Distributions for Different Climatic Zones in Tropical India. Progr. Electromagn. Res. B 25, 211–224. https://doi.org/10.2528/PIERB10072707.

Das, S., Chakraborty, M., Chakraborty, S., Shukla, A.K., Acharya, R., 2020. Experimental studies of Ka Band Rain Fade Slope at a Tropical Location of India. Adv. Space Res. 66 (7), 1151–1157.

Feral, L., Sauvageo, H., Castanet, L., Lemorton, J., 2003. HYCELL–A new hybrid model of the rain horizontal distribution for propagation studies: 1. Modeling of the rain cell. Radio Sci. 38 (3), 1056. https://doi.org/10.1029/2002RS002802.

Flavin, R.K., 1996. Satellite link rain attenuation in Brisbane and a proposed new model for Australia. Rep. 8375, Telstra Res. Lab., Clayton, Victoria, Australia, 15.

Feldhake, G.S., Sengers, L.A., 2002. Communication of multiple rain attenuation models with three years of Ka Band propagation data concurrently taken at eight different locations. Online J. Space Commun., 1–5

Gray, W.R., Seed, A.W., 2000. The characterization of orographic rainfall. Meteorol. Appl 7, 105–119.

García-López, J.A., Hernando, J.M., Selga, J., 1988. Simple Rain attenuation Method for Satellite Radio Links". IEEE Trans. Antennas Propag. 36 (3), 444–448.

ITU-R-R Recommendation P.838–3, 2005. Specific attenuation model for rain for use in prediction methods.

ITU-R Recommendation P.618-13, 2017. Propagation data and prediction methods required for the design of earth-space telecommunication systems.

ITU-R Recommendation P.618-8, 2003. Propagation data and prediction methods required for the design of Earth-space telecommunication systems.

ITU-R Recommendation P.618-12, 2015. Propagation data and prediction methods required for the design of Earth-space telecommunication systems.

ITU-R-R Recommendation P.839–3, 2001. Rain height model for prediction methods.

ITU-R Document 3M/17. Comments on Recommendation ITU-R P.618-7 Propagation data and prediction methods required for the design of Earth-space telecommunication systems, Brazil, 2003.

ITU-R Document 3J/50. Recommendation ITU-R P.618-9 rain attenuation prediction: prediction for low latitudes and low elevation", ESA, Italy, 2008.

Kubista, E., Fontan, F.P., Castro, M.A.V., Buonomo, S., Arbesser-Rastburg, B.R. Baptista, and J.P. Baptista, 2000. Ka-band propagation measurements and statistics for land mobile satellite applications, IEEE Trans. Vehicular Technol., vol. 49(3): 973–983, doi: https://doi.org/10.1109/25.845114.

Karmakar, P.K., Chattopadhyay, S., Sen, A.K., 2000. Radiometric measurements of rain attenuation and estimation of rain height. Indian J. Radio Space Phys. 29, 95–110.

Luini, L., Capsoni, C., 2011. MultiEXCELL: a new rain field model for propagation applications. IEEE Trans. Antennas Propagat. 59 (11), 4286–4300.

Maitra., 2004. Rain attenuation modeling from measurements of rain drop size distribution in the Indian region. IEEE Antennas Wireless Propagat. Lett., vol. 3:180-181, doi: https://doi.org/10.1109/LAWP.2004.833979.

Matricciani, E., 2008. 18.7 GHz tropospheric scintillation and simultaneous rain attenuation measured at Spino d'Adda and Darmstadt with Italsat. Radio Sci., 43(1): RS 1013, 1–13.

Mishra, M.K., Renju, R., Mathew, N., Raju, C.S., Sujimol, M.R., Shahana, K., 2020. Characterization of GSAT-14 satellite Ka-band microwave signal attenuation due to precipitation over a tropical coastal station in the southern peninsular region of the Indian subcontinent. Radio Sci. 55 (2), 1–9. https://doi.org/10.1029/2019RS006910.

Mulangu, C.T., Afullo, T.J., 2009. Variability of the propagation coefficients due to rain for microwave links in southern Africa. Radio Sci. 44 (3), 1–10. https://doi.org/10.1029/2008RS003912.

Panchal, P., Joshi, R., 2016. Performance Analysis and Simulation of Rain Attenuation Models at 12–40 GHz Band for an Earth Space Path over Indian Cities. Procedia Comput. Sci. 79, 801–808.

Ramachandran, V., Kumar, V., 2007. Modified rain attenuation model for tropical regions for Ku-band signals. Int. J. Satell. Commun. Network. 25 (1), 53–67.

Rice, P.L., Holmberg, N.R., 1973. Cumulative time statistics of surface-point rainfall rates. IEEE Trans. Commun. 21 (10), 1131–1136.

Samat, F., Jit Singh, M.S., Sountharapandian, T., 2019. Rain Attenuation Prediction Model Assessment on 3-Year Ka-Band Signal of MEASAT-5 at Tropical Region Using 7.3-m Antenna. MAPAN 35, 201–212.

Sheng, N., C., Lin, W., Zhang, Q., Bai, R., 2014. Modelling of millimeter wave propagation in rain based on parabolic equation method. IEEE Antennas Wireless Propagat. Lett. 13: 3-6.

Stutzman, W.L., Yon, K.M., 1986. A simple rain attenuation model for earth–space radio links operating at 10–35 GHz. Radio Sci. 21 (1), 65–72.

Tjelta, T., Rytir, M., Braten, L.E., Grotthing, P.A., Cheffena, M., Hakegard, J.E., 2017. Results of a Ka band campaign for the characterisation of propagation conditions for SatCom systems at high latitudes. In: 2017 11th European Conference on Antennas and Propagation (EUCAP), pp. 1481–1485. https://doi.org/10.23919/EuCAP.2017.7928507.lui.

Yamada, M., Karasawa, Y., Yasunaga, M., Arbesser-Rastburg, B., 1987. An improved prediction method for rain attenuation in satellite communications operating at 10–20 GHz. Radio Sci. 22 (6), 1053–1062.

Yeo, J.X., Lee, Y.H., Ong, J.T., 2014. Rain Attenuation Prediction Model for Satellite Communications in Tropical Regions. IEEE Trans. Antennas Propag. 62 (11), 5775–5781.

https://www.itu.int/dms_pubrec/itu-r/rec/p/R-REC-P.837-4-200304-S!!PDF-E.pdf 837(4) .